

Supporting Information for:

High-Performance Flexible Asymmetric Supercapacitors Based on 3D Porous Graphene/MnO₂ Nanorod and Graphene/Ag Hybrid Thin-Film Electrodes

Yuanlong Shao,^a Hongzhi Wang,^{*a} Qinghong Zhang^b and Yaogang Li^{*b}

^a State Key Laboratory for Modification of Chemical Fibers and Polymer Materials, College of Materials Science and Engineering, Donghua University, Shanghai 201620, P. R. China.

^b Engineering Research Center of Advanced Glasses Manufacturing Technology, Ministry of Education, College of Materials Science and Engineering, Donghua University, Shanghai 201620, P. R. China.

Characterization of MnO₂ nanorod.....	2
Extra characterization of graphene/MnO₂ hybrid films.....	4
Characterization of graphene/Ag composite.....	5
Raman and FTIR spectroscopy measurement of GO, graphene, graphene/MnO₂ and graphene/Ag.....	7
Electrochemical measurement of graphene/MnO₂ hybrid films.....	9
Comparison of the specific capacitance of two asymmetric systems.....	11
Cycle performance of the graphene/MnO₂//graphene/Ag asymmetric supercapacitor.....	12
Comparison of N₂ BET data for graphene/MnO₂ hybrid film, graphene/Ag hybrid film and graphene film.....	13
References.....	14

Characterization of MnO₂ nanorod

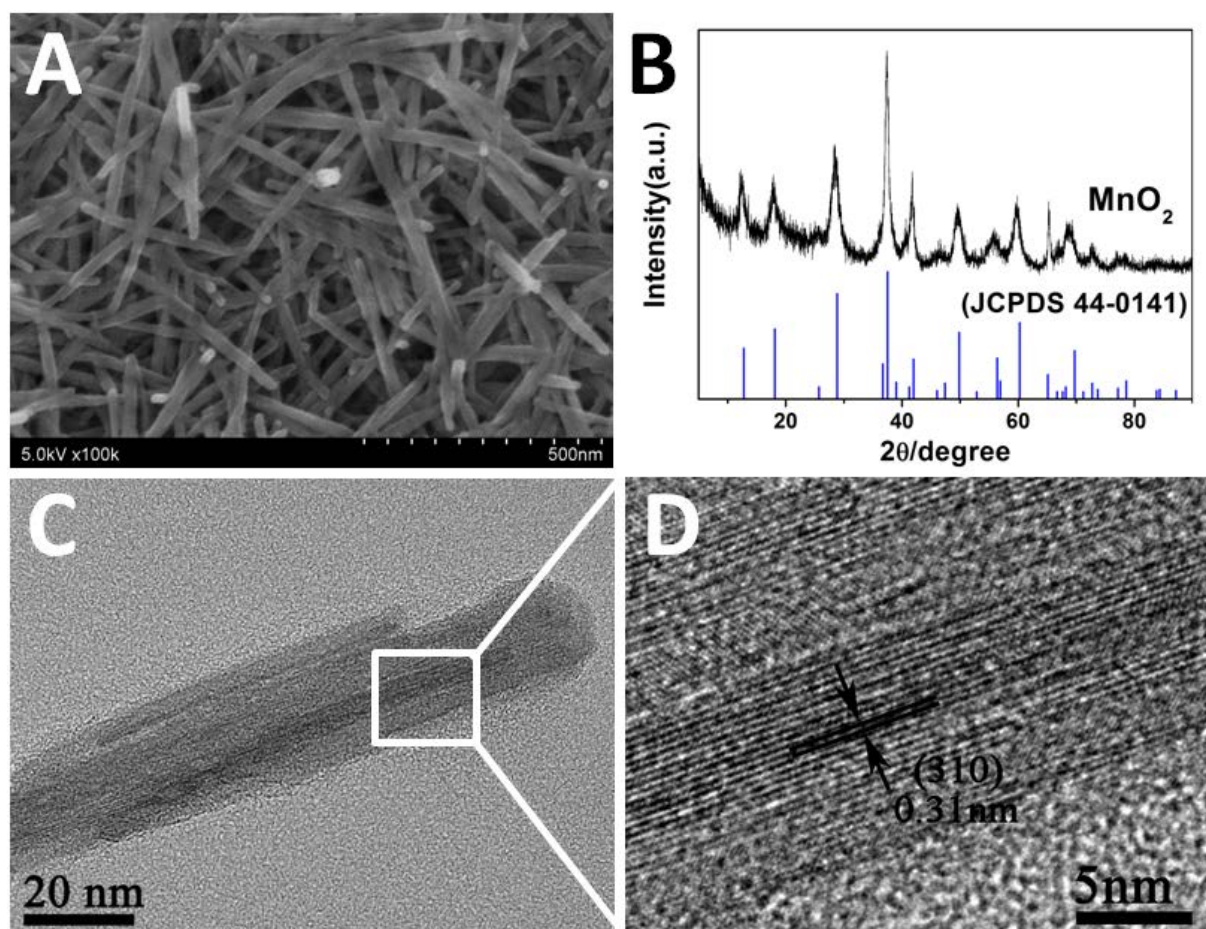


Figure S1. (A) FE-SEM of MnO₂ nanorod with diameter of 30 nm and length of 300-400 on average. (B) TEM image of single MnO₂ nanorod. (C) High-resolution TEM of the selected area. (D) Typical XRD spectrum of MnO₂ nanorod.

Figure S1A shows the typical field emission scanning electron microscopy (FE-SEM) image of MnO₂ nanorod. As can be seen from the Figure S1A, MnO₂ nanorod have uniform diameters of 30nm and length of 300–400nm, which are in agreement with the transmission electronic micrographs (TEM) image (Figure S1B). In the corresponding high-resolution (HR)-TEM image (Figure S1C), exhibits obvious crystalline structures with a very good lattice fringe, corresponded to a d-spacing of 0.31nm, which can be indexed as the (310) plane of the α -phase MnO₂. Further information on the composition of the as-prepared MnO₂ nanorod was obtained by the X-ray diffraction (XRD) measurements (Figure S1D). The XRD pattern of the nanorod corresponded well

with standard pattern of α -MnO₂ (JCPDS, PDF-44-0141), which have monoclinic structure with A2/m space group and lattice constants of $a=9.7845\text{\AA}$ and $c=2.8630\text{\AA}$ ^[S1]. Furthermore, no extra peaks attributable to manganese oxides with other crystallographic forms are observed, which indicates the highly purity and crystalline nature of the MnO₂ nanorod and is in agreement with the HR-TEM observations.

Extra characterization of graphene/MnO₂ hybrid films

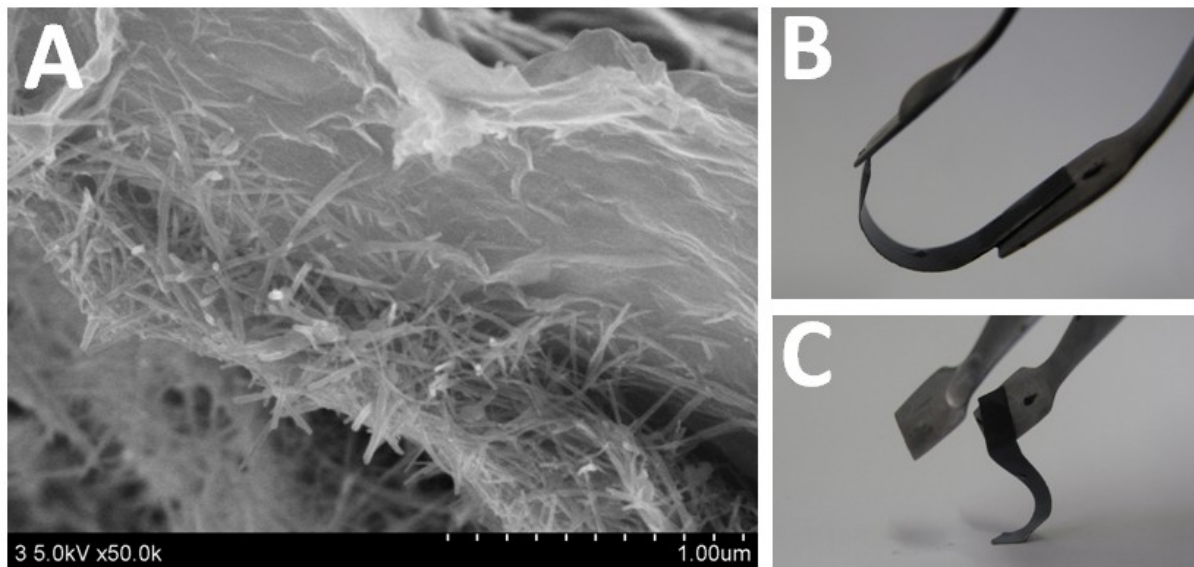


Figure S2. (A) SEM of stripped graphene/MnO₂ film. (B, C) Digital images of bent flexible graphene/MnO₂ hybrid films.

Characterization of graphene/Ag composite

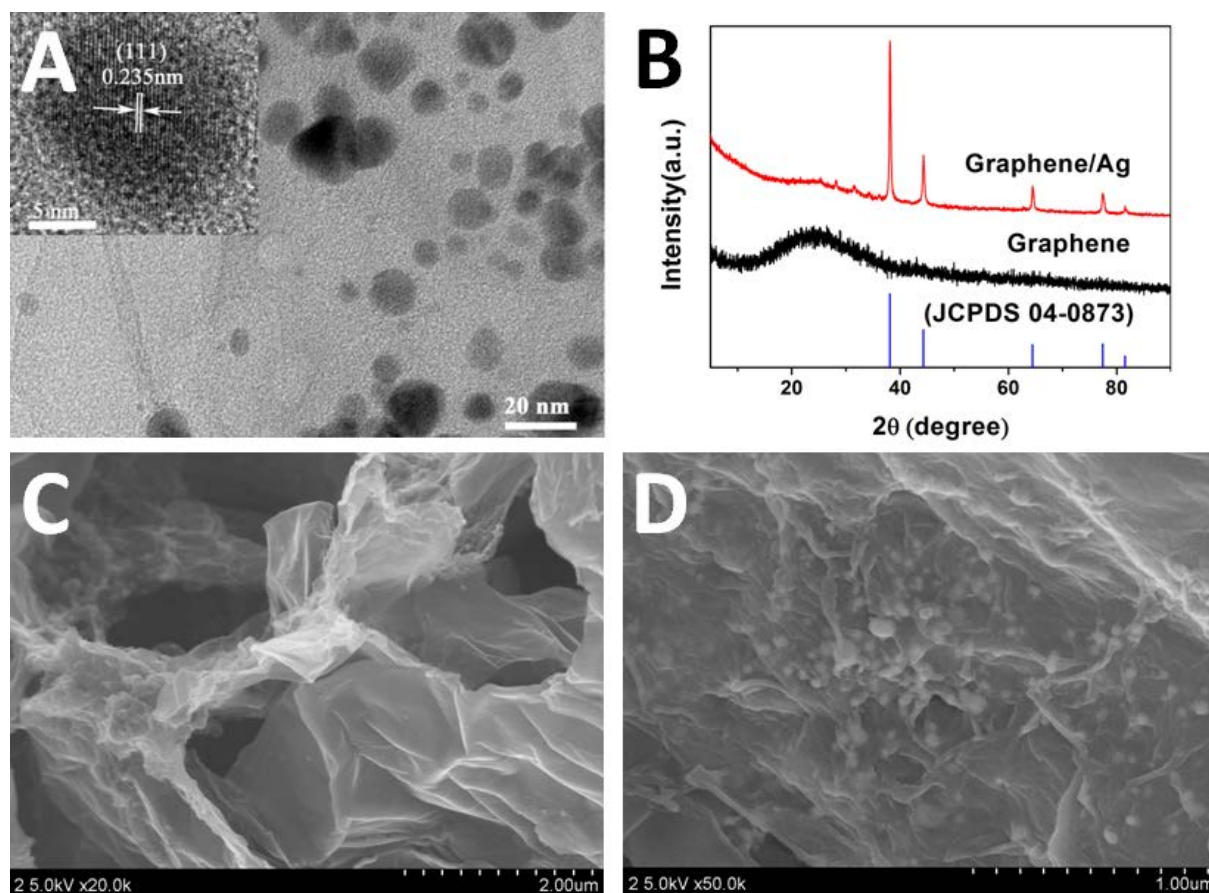


Figure S3. (A) TEM image of graphene/Ag composite, and HRTEM of Ag particle in the graphene/Ag composite (inset), (B) XRD patterns of graphene, and graphene/Ag composite, Different parts SEM images of graphene/Ag films interior microstructures: (C) micropores of the graphene/Ag network, (D) Walls of micropores.

Characteristic TEM micrograph as shown in **Figure S3A** shows uniform single entity Ag nanoparticles (5-20nm) embed in the Graphene sheets. The presence of the bigger particles can be attributed to agglomeration of smaller particles. Graphene sheets exhibit a smooth finish and plenty of wrinkles, owing to the thin structure of the sheet. The HRTEM micrograph of Ag nanoparticle decorated on graphene sheets is shown in the inset graph of Figure S3A, where a very good lattice fringe of Ag crystal structure is well-resolved. The measured lattice fringe spacing of 0.235 nm in these Ag nanoparticles corresponds to the (111) crystal plane. Figure S3B shows the XRD patterns of

graphene and graphene/Ag composite. The XRD patterns also confirmed the crystalline structure of nanoparticles decorated on graphene sheets to be Ag (JPCDS, PDF 04-0873). Except for the broad diffraction peak of graphene, there is no extra peak observed in the XRD spectrum, which confirms the highly crystallinity of Ag nanoparticles and is in agreement with the HRTEM observations.

Raman and FTIR spectroscopy measurement of GO, graphene, graphene/MnO₂ and graphene/Ag

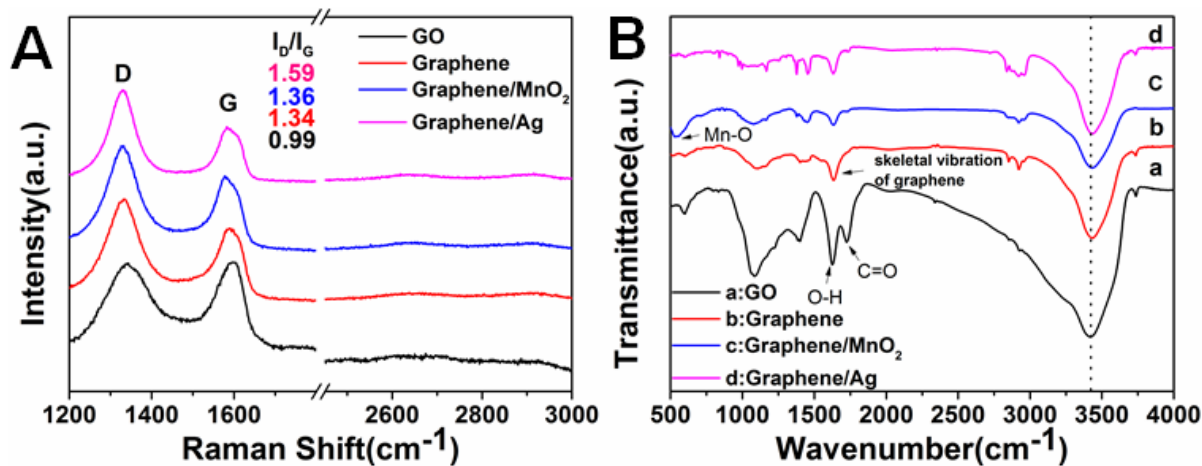


Figure S4. (A) Raman spectra of GO, Graphene, Graphene/MnO₂, and Graphene/Ag; (B) Comparison of FTIR spectra of GO, Graphene, Graphene/MnO₂, and Graphene/Ag.

Figure S4A shows the Raman spectra of GO, graphene, graphene/MnO₂, and graphene/Ag, which exhibit two typical peaks. For GO sample, the well-known G band at 1585 cm⁻¹ is characteristic for sp²-hybridized C-C bonds in a two-dimensional hexagonal lattice. While the D band located at 1335 cm⁻¹ corresponds to the defects and disorder carbon in the graphite layers. The ratio of the intensity of the D band and G band (I_D/I_G) changes from 0.99 (GO) to approximately 1.35 (graphene, graphene/MnO₂), manifesting a trend of decrease in the average size of the sp² domains upon the reduction of GO [S2]. Moreover, the I_D/I_G of graphene/Ag is 1.59, even larger than that of graphene, which indicates the increased surface defects because of the Ag nanoparticles decorated on the surface of graphene.

In order to further confirm the reduction mechanism of the composites, FT-IR analyses of GO, graphene, graphene/MnO₂, and graphene/Ag were performed and the corresponding spectra are shown in Figure S4B. The most significant absorption peaks at around 3500cm⁻¹ can be assigned to O-H stretching vibrations due to the hydroxyl groups. The dampening and subsequent shift of the peak shows the involvement of the O-H group in the reduction. Absorptions due to the C=O group (1725 cm⁻¹) are decreased obviously in intensity and the absorptions at 1635 cm⁻¹ (O-H groups) are absent, suggesting that the carboxyl groups on the surface of GO have been reduced or modified by

Ag particles. Furthermore, two new peaks located at 563 cm^{-1} occurred in the spectra of graphene/MnO₂, which can be ascribed to the Mn-O vibrations^[S3].

Electrochemical measurement of graphene/MnO₂ hybrid films

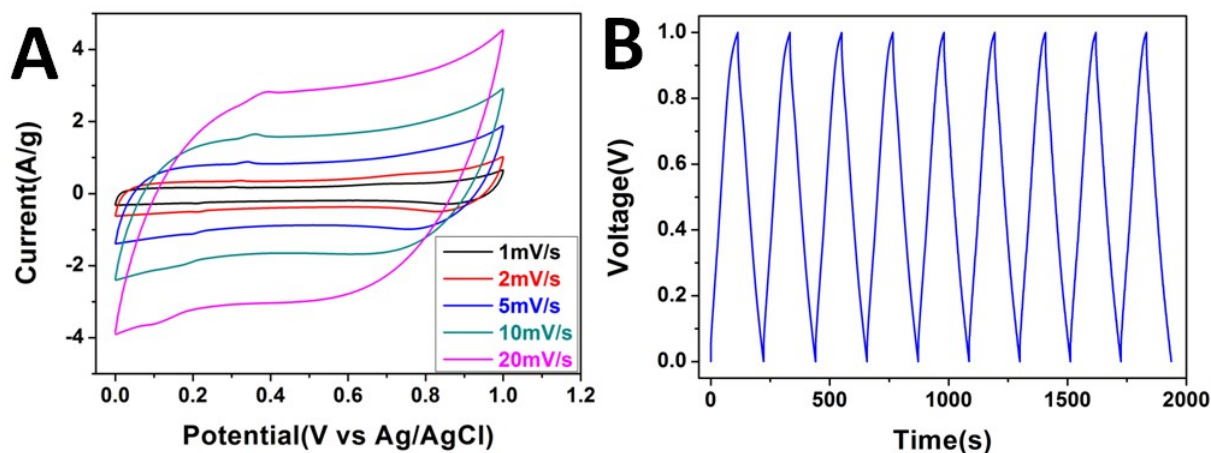


Figure S5. Electrochemical measurement of graphene/MnO₂ film using 1M Na₂SO₄ aqueous solution as electrolyte in a three-electrode configuration. (A) Cyclic voltammeter curves with different scan rates, (B) Galvanostatic charging/discharging curves measured with a current density of 1A g⁻¹.

To evaluate the electrochemical properties and quantify the specific capacitance of the graphene/MnO₂ films, the electrochemical measurements were carried out using 1M Na₂SO₄ aqueous solution as electrolyte in a three-electrode configuration, in which an Ag/AgCl (saturated KCl) assembly and a platinum wire were used as the reference electrode and the counter electrode, respectively. We performed cyclic voltammetry (CV) measurements to evaluate the stability and the electrochemical behavior of graphene/MnO₂ films within a potential window of 0.0 to 1.0V. The specific capacitance of the graphene/MnO₂ films was calculated from the CV results. This hybrid films exhibit high specific capacitance of 209F g⁻¹. **Figure S5A** shows the CV measurements results of graphene/MnO₂ films at scan rates of 1, 2, 5, 10, and 20mV s⁻¹, which exhibit quasi-rectangular shape of these curves. The shape of the CV curves of is different from electrical double-layer (EDL) capacitor because the overall capacitance derives from the combined contribution of the main redox pseudocapacitance of MnO₂ and partly from the EDL capacitance of graphene in the composite. Furthermore, the CV curve of the graphene/MnO₂ film electrode exhibits nearly a mirror-image current response on voltage reversal, meaning ideal capacitive behavior. The galvanostatic

charging/discharging curves of the graphene/MnO₂ film are highly linear and symmetrical, indicating a rapid I-V response and a good reversibility.

Comparison of the specific capacitance of two asymmetric systems

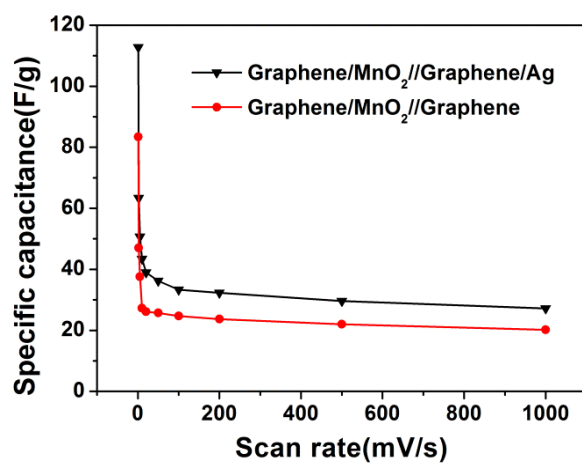


Figure S6. Comparison of the specific capacitance of graphene/MnO₂//graphene/Ag and graphene/MnO₂//graphene asymmetric supercapacitor with different scan rates.

Cycle performance of the graphene/MnO₂//graphene/Ag asymmetric supercapacitor

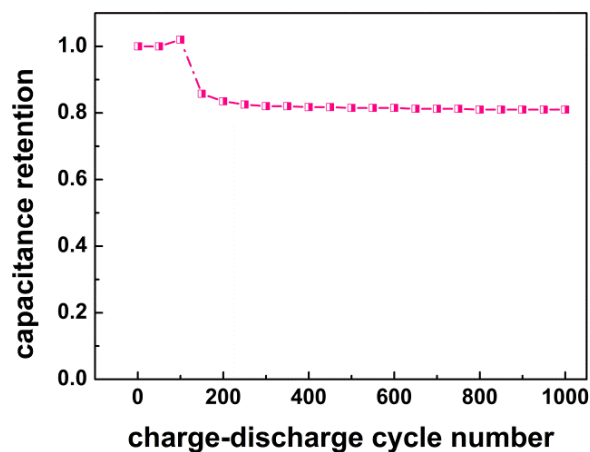


Figure S7. Cycle performance of the graphene/MnO₂//graphene/Ag asymmetric supercapacitor with a voltage of 1.8 V at a current density of 2.2 A g⁻¹ in 1 M Na₂SO₄ aqueous solution.

The cycling performance test for the graphene/MnO₂//graphene/Ag asymmetric SC was carried in the voltage window from 0 to 1.8 V at a current density of 2.2 A g⁻¹. **Figure S7** exhibits the capacitance retention ratio of the asymmetric capacitor charged as a function of the cycle number. After 1000 cycles, the specific capacitance retains about ~81% of the initial capacitance. It was assumed that the capacitance decline is according to the corrosion of the current collector caused by the dissolved oxygen in electrolytes together with the excessive positive potential on the MnO₂ and/or matching problem^[S4]. We believe that the cycling performance of graphene/MnO₂//graphene/Ag asymmetric SC can be further improved via removal of dissolved oxygen in the aqueous electrolyte and optimizing capacitor parameters (such as current density and potential matching), volume ratio of the two electrodes, and the ion concentration^[S4].

Comparison of N₂ BET data for graphene/MnO₂ hybrid film, graphene/Ag hybrid film and graphene film

Table 1 The textural properties of graphene/MnO₂, graphene/Ag hybrid films and graphene film after freeze-drying and vacuum drying

Sample name	S _{BET} (m ² g ⁻¹)	D _{ads} ^a (nm)
Graphene/MnO ₂ film	11.6	72.6
Graphene/Ag film	11.5	30.9
Graphene film	2.9	-

^aThe pore size derived from adsorption branch.

To get the values of specific area from BET, the samples are subjected to freeze-drying and vacuum drying. During the drying process, the graphene sheets in the hybrid films are drastically shrunked, which result in substantial decline in the specific surface area. The undried hybrid graphene films must process larger specific area. The resulting BET specific area of graphene/MnO₂ nanorods and graphene/Ag hybrid films is 11.6 m² g⁻¹ and 11.5 m² g⁻¹ respectively, in contrast to 2.9 m² g⁻¹ for graphene film; this reflects the higher surface area achieved with the graphene/MnO₂ and graphene/Ag films. Compared with the specific area for graphene/Polyaniline nanofiber composite films (12.7 m² g⁻¹)^[S5], the obtained specific area of hybrid films are reliable.

References

- [S1] S. Chen, J. Zhu, Q. Han, Z. Zheng, Y. Yang, X. Wang, *Cryst. Growth Des.*, 2009, **9**, 4356.
- [S2] J. I. Paredes, S. R. Villar, P. F. Solis, A. A. Martinez, M. J. Tascon, *Langmuir*, 2009, **25**, 5957.
- [S3] Z. P. Li, Y. J. Mi, X. H. Liu, S. Liu, S. R. Yang, J. Q. Wang, *J. Mater. Chem.*, 2011, **21**, 14706.
- [S4] Z.S. Wu, W. Ren, D. W. Wang, F. Li, B. Liu, H. M. Cheng, *ACS Nano*, 2010, **4**, 5835.
- [S5] Q. Wu, Y. X. Xu, Z.-Y. Yao, A. R. Liu, G. Q. Shi, *ACS Nano*, 2010, **4**, 1963.